An Improved Electroporator With Continuous Liquid Flow and Double-Exponential Waveform for Liquid Food Pasteurization

RAI NAVEED ARSHAD[ID][1]**, ZULKURNAIN ABDUL-MALEK**[ID][1]**, (Senior Member, IEEE),
ABDULLAH MUNIR**[1,2]**, MOHD HAFIZI AHMAD**[1]**, (Member, IEEE), ZAINUDDIN NAWAWI**[3]**,
MUHAMMAD ABU BAKAR SIDIK**[3]**, (Member, IEEE), TOUQEER A. JUMANI**[ID][4]**,
ILYAS KHAN**[ID][5]**, HAMMAD ALOTAIBI**[6]**, AND AFRASYAB KHAN**[7]

[1]Faculty of Engineering, School of Electrical Engineering, Institute of High Voltage and High Current (IVAT), Universiti Teknologi Malaysia, Johor Bahru, Johor 81310, Malaysia
[2]Department of Electrical Engineering, NED University of Engineering and Technology, Karachi 75270, Pakistan
[3]Department of Electrical Engineering, Faculty of Engineering, Universitas Sriwijaya, Palembang, Sumatera Selatan 30662, Indonesia
[4]Department of Electrical Engineering, Mehran University of Engineering and Technology, SZAB Campus, Khairpur Mirs 66020, Pakistan
[5]Department of Mechatronics and System Engineering, College of Engineering, Majmaah University, Majmaah 11952, Saudi Arabia
[6]Department of Mathematics, College of Science, Taif University, Taif 21944, Saudi Arabia
[7]Department of Vibration Testing and Equipment Condition Monitoring, Research Institute of Mechanical Engineering, South Ural State University, 454080 Chelyabinsk, Russia

Corresponding authors: Ilyas Khan (i.said@mu.edu.sa) and Zulkurnain Abdul-Malek (zulkurnain@utm.my)

ABSTRACT Pulsed electric field (PEF) pasteurisation keeps treated liquid food fresh and nutritious compared to traditional thermal pasteurisation. However, PEF adoption is still limited on an industrial scale due to a lack of practical systems. As a result, a great deal of research has gone into overcoming the limitations of the existing systems. Keeping this in mind, the current study contributes to the improvement of the electroporator. The heterogeneous electric field's distribution raises the temperature of the treated food samples. Liquid laminar flow is a reason for heterogeneous electric field's distribution in continuous treatment. Hotspots may also be created by using an inefficient high-voltage waveform in addition to the heterogeneous electric field distribution. This study rectifies the heterogeneous distribution by proposing an improved coaxial treatment chamber and double-exponential waveform to replace the exponential-decaying waveform. A static mixer provides an increased mixing, i.e. disrupting the laminar flow, inside the treatment zone. COMSOL based computational model was developed to study flow behaviour and corresponding temperature distribution in the proposed coaxial treatment chamber with sieves. Based on the model, it has been concluded that coaxial electrodes with sieves provide more homogeneous flow properties inside the treatment chamber. The effectiveness of the double-exponential (DE) waveform was validated using MATLAB. A three-stage Marx generator giving the DE waveform was designed and constructed. The performance of the improved treatment chamber together with the DE waveform, known as the electroporator, was studied using chemical and microbial analysis. Untreated, PEF treated, and thermal treated orange samples were stored at 4°C for 9 days before being examined. The lowest microbial growth was observed in both the PEF treated with sieves and thermally treated food samples than the untreated sample. However, treated juices' visual and chemical colour analysis showed that the PEF-treated sample acquired a brighter appearance than a thermally processed sample. Thus, this study provides significant findings in developing and utilising an electroporator to inactivate microorganisms.

INDEX TERMS COMSOL, continuous flow, double-exponential waveform, laminar flow, liquid food treatment, static mixer.

The associate editor coordinating the review of this manuscript and approving it for publication was Rajeeb Dey[ID].

I. INTRODUCTION

There are various applications for electrical energy in the food industry, especially in processing and preservation.

The most common ones are ohmic heating, microwave heating, high-voltage arc discharge, low electric field stimulation and high-intensity pulsed electric field (PEF) [1]. Ohmic heating is an example of thermal treatment and damages the food products, which affects the taste, flavour, and nutrient contents of the food. Therefore, researchers have strived to develop non-thermal food treatment techniques as an alternative to conventional thermal treatments [2], [3]. As a result, PEF technology has gained popularity in the food industry since it offers unique food safety benefits, nutritional preservation and low energy usage compared to thermal treatment [4].

A typical PEF processing system includes a high-voltage pulse generator, one or more treatment chambers, control and monitoring units [5]. Electric field intensity, treatment time, pulse shape, pulse width, and pulse frequency are essential parameters that substantially affect process efficiency [6]. The development of the PEF system for efficient treatment procedures has been evolved as an interesting research domain over the past decade [7]. PEF treatment now outperforms conventional thermal food processing because of the developments in power electronics [4]. As a result, the research on solid-state pulsed power generators has proposed different treatment protocols for PEF processing.
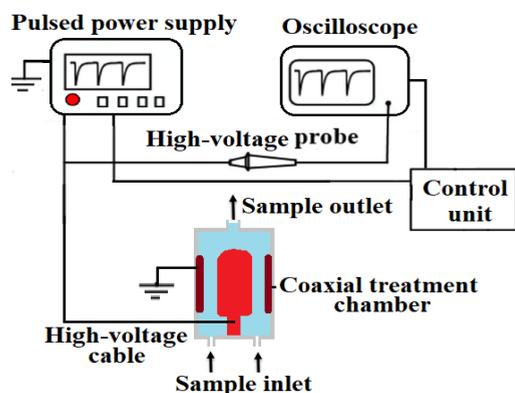
FIGURE 1. A block diagram of the PEF system containing a coaxial treatment chamber.

The treatment chamber is an integral part of the PEF system for liquid food pasteurisation, consisting of electrodes fixed by an insulator [8]. As shown in Figure 1, a high voltage is delivered to the target biological cell placed inside the treatment chamber to initiate electroporation. A variety of static and continuous treatment chambers have been extensively explored [9], [10]. However, static processing is not suitable for bulk treatment since it is more expensive and time-consuming than continuous processing. In addition, treatment chambers may also be categorised according to the direction of the electric field and the flow of sample food. Parallel plate, coaxial, and co-linear chambers are the three most common chamber designs for PEF treatment.

In continuous PEF processing, an adequately designed treatment chamber with uniform field strength may effectively kill or weaken the microorganism in the juices. Homogeneous distribution of electric field is dependent on the design of the treatment chamber [11]. The chamber design may be modified by rearranging electrodes or insulator material in the flow channel according to the application. The flow rate is an interdependent parameter in PEF treatment and plays a crucial role in this process. References [12], [13] investigated the geometry of the treatment zone and flow rate for the liquid food using a continuous co-linear PEF system. It was found that a laminar liquid flow is a cause of heterogeneous treatment. High power and high-frequency pulse generator can deliver a required amount of energy per unit volume to the whole target sample to accommodate the laminar flow in the processing zone [14]. However, it complicates the development of the electrical system.

A static mixer can provide intensive fluid mixing by generating artificial turbulence inside the treatment zone [15]. It eventually results in a more uniform temperature and electric field distribution throughout the whole sample being treated. This static mixing produces higher friction of particles, boosting heat transfer compared to laminar flow [5], [13]. This static mixing can be accomplished by adding certain physical obstacles into the treatment zone [16], [17]. As a result, it is much more interesting and beneficial to study the dynamics of laminar flow and fluid mixing effects using computational fluid dynamics (CFD) [5].

A coaxial treatment chamber equipped with a static mixer was developed in this study to provide uniform flow and electric field distribution. Firstly, the optimal size and capacity of the chamber were established. Secondly, the proposed treatment chamber was evaluated using COMSOL Multiphysics software. Thirdly, the necessary voltage and current for electroporation were calculated, and a Marx generator with DE waveform was constructed. Finally, the proposed electroporator was assessed through a microbial and chemical test of the treated orange juice. Additionally, the findings of the tests were compared to those of thermally treated juice samples.

II. COAXIAL TREATMENT CHAMBER FABRICATION
It is essential to do an accurate design study of the treatment chamber to determine the electric field distribution inside the treatment zone and design the required high voltage pulse generator.

A. GEOMETRICAL PARAMETERS
Coaxial treatment chambers can successfully yield accurate characterised electric field distribution for medium-sized volumes [18]. The coaxial treatment chamber has been recommended due to its straightforward design and adjustable impedance for the various conductivities of the sample food. Some measures must be taken to maintain resistance and minimum fluctuations in the intensities of the electric field in the treatment area [19]. There should be no electrodes with sharp edges since the electric field increases on these sharp edges, causing arcing within the liquid food [20].
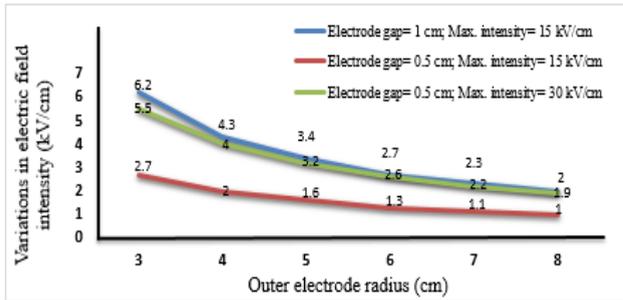
FIGURE 2. Variation of the electric field in the treatment zone with different electrodes' radii, the gap between electrodes and the applied voltage.

FIGURE 3. Resistance of coaxial treatment chamber with different length, electrode radii and the gap between electrodes.

The electrical field strength is the strongest near the electrode region in the coaxial treatment chamber coupled with the high voltage supply [16]. The field strength within any location at 'r', such that $R_1 < r < R_2$, is known through the following equation (1):

$$E = \frac{V}{r \ln\left(\frac{R_o}{R_i}\right)} \quad (1)$$

where R_i and R_o are the radii of the inner and outer electrodes, respectively. Equation 1 is applicable only when radii do not exceed the chamber's length [21]. Using equation 1, figure 2 plots the electric field variation in the treatment zone with different electrodes' radii, the gap between electrodes, and the applied voltage. It shows that electric field inhomogeneity can be reduced by decreasing the gap between the electrodes. However, it hinders the volume of a large industrial plant. Therefore, to keep the chamber's outer volume reasonably small and at the same time allow a sufficient volume, an outer electrode with a radius of 3.0 cm has been selected for the proposed design.

The treatment chamber's electrical impedance is another critical parameter for designing its pulse generator [5]. A coaxial treatment chamber with a liquid food sample can be modelled using a parallel arrangement of resistance and a capacitor [21]. In this model, the resistance is insignificant compared with the capacitance resulting from which the load can be perceived as a pure resistive. Electrodes' physical dimensions and the liquid food sample's conductivity are the principal critical parameters influencing electrical impedance. The equivalent resistance and capacitance for a coaxial configuration can be calculated as:

$$R = \frac{\ln\left(\frac{R_o}{R_i}\right)}{2\pi \sigma l} \quad (2)$$

where the treatment chambers' length '*l*' and the sample food conductivity (σ) are decisive parameters in designing the treatment chamber's dimensions. Food's conductivity is, temperature-dependent; it rises with the rise of temperature; consequently, increases with the thermal energy dissipated into the sample. As a result, the chamber's resistance decreases, drain more current from the pulse generator
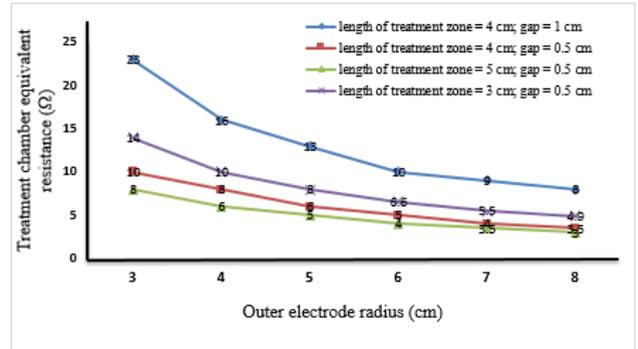
and the wave shape of the applied pulsed generator also changes.

Usually, a lengthy treatment chamber is favourable for increasing the treatment time and avoiding long due to undesirable overheating [22]. However, figure 3 shows that the coaxial treatment chamber's electrical resistance decreases with the length of the treatment zone for a fixed electrode gap. Consequently, a higher-current power supply is required, posing additional supply design challenges [5]. Similarly, figure 3 also shows that chamber resistance increases with increasing the electrodes gap and radii. However, as seen in Figure 2, this requirement contradicts the radial fluctuations of electric field intensity. As a result, an appropriate design must be chosen to satisfy these two limitations. Therefore, the following dimensions of the treatment chamber have been finalised to accommodate the requirements as mentioned above:

- Length of treatment zone: $l = 3$ cm
- Outer electrode's radius: $R_o = 3$ cm
- Inner electrode's radius: $R_i = 2.5$ cm
- Gap between electrodes: 0.5 cm

Then the volume of this cylinder = 26ml, and these dimensions give a resistance of 5 Ω with orange juice.
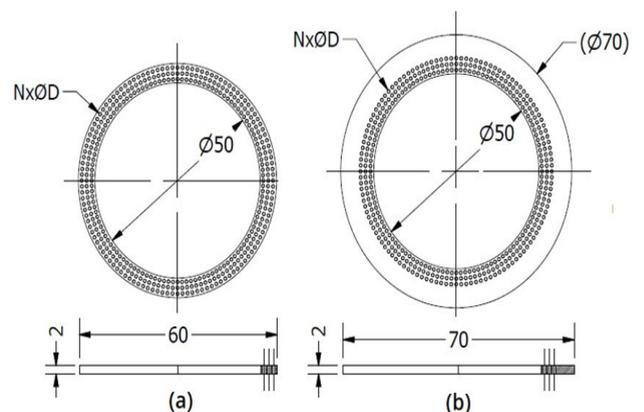
FIGURE 4. Sieve geometries used as a static mixer in the design, (a) lower sieve, (b) upper sieve.

B. DESIGNING STATIC MIXER

Static mixers are special mixing tools used in the chemical process industry for in-line mixing [23]. Static mixers have certain benefits, such as increasing heat dissipation and mass transfer without external resources, low maintenance costs, short residence time and limited space [24], [25]. The sieves for the proposed coaxial treatment chamber were constructed in two distinct sizes to fit in the proposed assembly, as shown in Figure 4. One mesh was a circular ring with an inner and outer radius of 2.5 and 3.0 cm (Figure 4.a). A second was made of a circular ring with inner and outer radii of 2.5 and 3.5 cm (Figure 4.b). These sieves were contained circular holes with 0.5 mm diameter, whereas the insulator thread of the mesh electrode was 0.15 mm wide. Figure 5 shows the whole mechanical assembly of the proposed treatment chamber with sieve-1 and sieve-2.
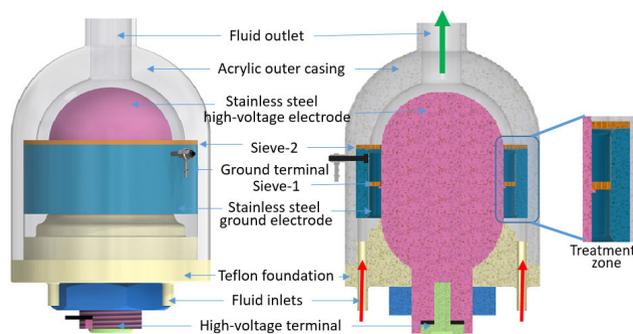
FIGURE 5. Mechanical design of the proposed treatment chamber.

C. MATERIALS OF THE CHAMBER

Table 1 lists the model's materials and their major characteristics. Electrodes' physical properties, such as surface roughness and accumulation of biological matter like protein or fat deposits, also affect the electrodes' characteristics [26]. The electrodes were stainless steel, while the insulator base was Teflon (Polytetrafluoroethylene - PTFE). Acrylic was used for both the mesh and the exterior casing since it is transparent and lightweight.

Stainless steel resistance to corrosion was the main reason for choosing it. Stainless steel's benefits for this project are ease of manufacture, high strength, cleanliness, ease of cleaning, long life cycle, and recyclable nature. Teflon was chosen for its nonstick properties because it is simple to clean. Teflon also has the following properties: it is chemically inert (not chemically reactive), it may be utilised at temperatures ranging from −200 °C to +260 °C, it has a high electrical resistance, and it has high dielectric strength.

III. COMSOL SETUP FOR SIMULATION

Computational modelling is thus necessary owing to significant changes in the distribution, temperature and speed profile of electrical fields. [27]. It is possible to visualise the process variables by utilising computer modelling combined with fluid dynamics, electrical, and thermal problems associated with the treatment chamber.

TABLE 1. Materials and properties of different domains used in the simulation.

Symbol	Quantity	Conversion	Units
Electrodes Stainless steel (BS 460B)	Electrical conductivity (σ)	1.1x10⁶	S/m
	Thermal conductivity (k)	44.5	W/m K
	Thermal capacity (Cp)	475	J/kg K
	Density (ρ)	7850	kg/m³
Test material (orange juice)	Electrical conductivity (σ)	0.343	S/m
	Relative permittivity	30	
	Thermal capacity (Cp)	3730	J/kg K
Base insulator (Teflon)	Relative permittivity	2.1	
	Thermal conductivity (k)	0.24	W/m K
	Thermal capacity (Cp)	2200	J/kg K
	Density (ρ)	1050	kg/m³
Outer casing and sieves insulator (Coring 7740)	Relative permittivity	4.6	
	Thermal conductivity (k)	1.13	W/m K
	Thermal capacity (Cp)	753	J/kg K
	Density (ρ)	2230	kg/m³

The proposed treatment chamber was simulated in the COMSOL multiphysics (version 4.5). Therefore, it was necessary to adapt governing equations from COMSOL Multiphysics 4.5 to simulate the test chamber, which was accomplished using three modules: AC/DC for electrostatics, heat transfer for temperature analysis, and CFD for fluid dynamics research.
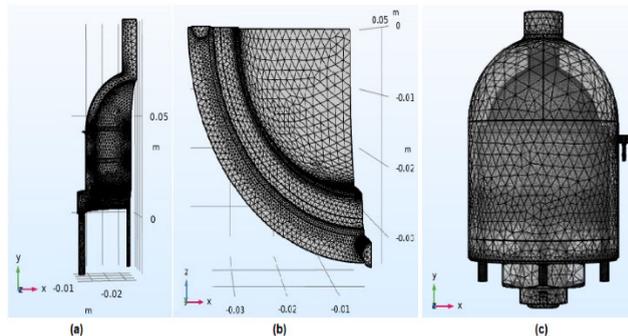
FIGURE 6. 2D view of meshing, (a) liquid domain in XY plane, (b) liquid domain in XZ plane (c) complete model in XY plane.

Figure 6 illustrates the proposed coaxial treatment chamber's simpler mesh structures. The geometry of the proposed treatment chamber was meshed with the "Fine" mesh to simulate in an acceptable amount of time. The most critical component has guaranteed that the minimum element size is less than the mesh size to get the highest possible resolution of the fine elements.

A. APPLIED PULSE WAVEFORM

PEF treatment aims to deliver the same amount of energy to all treatments, and it may be accomplished in various ways by adjusting the pulse parameters appropriately. In principle, many distinct pulses may be utilised for PEF treatment. The optimum pulse used in PEF treatment varies according to the cell's characteristics and cannot be defined as just one best answer.

PEF processing typically employs exponential-decaying (ED) and rectangular waveforms. Although the ED waveform is simple to create, it is the least efficient in PEF treatment. On the other hand, although a rectangular waveform is the most efficient, it is challenging to develop it. A double-exponential (DE) waveform is characterised by the difference of two exponentially decaying waveforms, which quickly reaches to peak value and then falls to zero. This waveform is commonly used in electromagnetic high power applications.
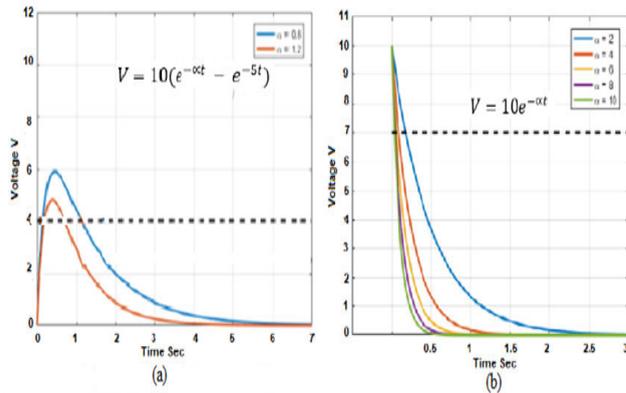
FIGURE 7. Simulation results showing efficiency comparison of two waveforms, (a) DE, (b) ED.

The efficiency of PEF to permeabilise biological cells is mainly dependent on the part of the applied pulses (time) during which the electric field strength exceeds a particular critical value [28]. Hence, a wider effective area of the applied waveform is recommended for electroporation, and this principle was used to measure the performance efficiency of ED and DE waveforms using Matlab. The efficiency of the waveform is defined as the ratio of the pulse area with a particular amplitude and duration over the total pulse area. Figure 7 shows the efficiency comparison of ED ($10e^{-\alpha t}$) and DE ($10(e^{-\alpha t} - e^{-\beta t})$) model waveforms. It shows that the efficiency of ED decreases with increasing the value of α, whereas it increases with increasing α in DE waveforms. Maximum efficiency (24%) was measured for the ED waveform, and 40% was observed for the DE waveform. Hence, DE is 1.7 times more efficient than the ED waveform.

Additionally, the DE waveform is wider than the ED waveform, which is also a prerequisite of the PEF treatment. The transformation of an ED waveform into an efficient DE waveform is accomplished using just a few passive electrical components [29]. Therefore, it lowers the power losses of the electrical system and can provide superior treatment at a reduced cost.

Table 2 shows the different parameters that were used to develop the DE waveform in the COMSOL model for the time-dependent testing of the proposed treatment chamber.

TABLE 2. Parameters of DE pulse generator used in COMSOL model.

Name	Expression	Value	Description
PW	1 [us]	1E^{-6} s	Pulse width DE waveform
Duty	10	10	Duty cycle
PP	PW/Duty*100	1E^{-5} s	Pulse period
PF	1/PP	1E5 1/s	Pulse frequency
lambda	c_const/PF	2997.9 m	wavelength
vel	1 [mm/s]	0.001 m/s	Initial liquid velocity
P-Amp	10 [kV]	10000 V	Pulse height
Ave	PW/PP*P-Amp	1000 V	Average applied voltage

B. ELECTRODE SHAPE

Sharp-edged electrodes may produce arcing since this sharp edge's surface density (charge per unit area) is considerably higher [9]. Therefore, the optimal electrode design was determined in static mode using 2D Comsol Multiphysics. Different shapes for the electrodes are illustrated in figure 8. In Figure 8, 'A' and 'B' are two stainless steel electrodes. 'A' and 'B' are the electrodes connected to the high voltage power source and the ground terminal, respectively.

A parametric sweep analysis of the electrodes' radius determined the optimal value for uniform electrical field distribution. Figure 8 demonstrates that rectangular and elliptical electrodes enhanced the electric field at the electrode's sharp edges. However, round-shaped electrodes (Figure 8.f) attains a maximum electric field of 35 kV.cm^{-1} compared to the rectangular and elliptical electrodes. Hence, the enhanced field may be reduced by increasing the sizes of the electrodes at the edges.

C. FLOW CHARACTERISTICS

The anticipated velocity profile was simulated using a circular treatment zone to simplify system modelling. The lowest
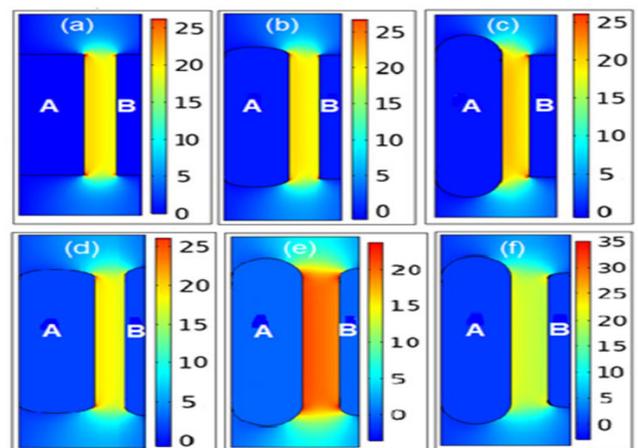
FIGURE 8. Simulation results showing predicted electric field distribution (kV.cm^{-1}) with different electrodes geometries of coaxial treatment chamber in 2D; A: high voltage electrode, B: Ground electrode; (a) A = rectangular, B = rectangular, (b) A = elliptical, B = rectangular, (c) A = circular, B = rectangular, (d) A = elliptical, B = elliptical; (e) A = circular, B = elliptical; (f) A = circular, B = circular.
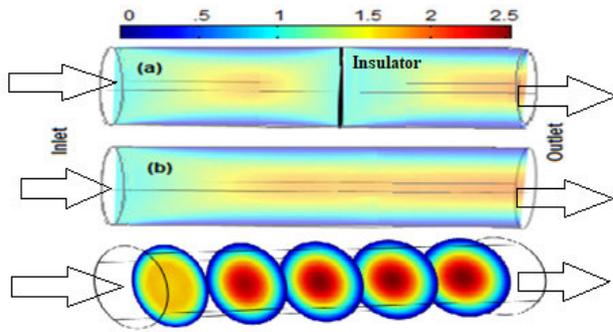
FIGURE 9. Simulation results showing 2D liquid velocity (mm/s) within the treatment chamber (a) with the sieve, (b) without sieve.

FIGURE 11. Line graph of the fluid velocity at different locations along a longitudinal axis from the mesh within the treatment chamber using inlet velocity 1mm/sec.

velocity of the fluid (1 mm.s^{-1}) was chosen at the circular pipe entry to measure the velocity profile. The highest flow velocity is observed at the centre of the flow path and decreases towards the walls, as seen in Figure 9. b. Hence, the liquid does not flow uniformly throughout the treatment zone. In Figure 9.a, an isolated mesh is placed in the pipe to overcome this constraint. The insulator geometry was intended to provide the least amount of flow resistance. As a result, the insulator does not reduce the pipe diameter any more than the other designs, resulting in faster flow rates.

Figure 10 illustrates the fluid velocity profiles recorded along the Y-axis at a distance of 1 cm from where the insulator was placed. Figure 10 demonstrates that the velocity profiles have a parabolic form without mesh, as anticipated from the laminar flow profiles shown in Figure 9. It also demonstrates that this parabolic shape was handled using a mesh inside the treatment zone. This fundamental idea was verified in simulations for every sample viscosity—inlet velocity on the flow profile corresponded with all the viscosity and treatment chamber configurations examined. Consequently, the parabolic velocity distribution grew as a consequence of the reduced intake velocity, which produced a laminar flow.

FIGURE 10. Line graph of fluid velocity within the treatment chamber along Y-axis with and without mesh.

As the distance from the sieves increases, the velocity profile takes on the form of a parabolic path, as shown in Figure 11. However, the velocity profile can overcome this parabolic profile to the distance of 1.2 cm from the mesh. Therefore, two sieves must be placed inside the 3-cm length of the proposed treatment zone to overcome the laminar flow and maintain uniformity in the velocity profile inside the treatment zone.

The liquid velocity profiles describe the residence time inside the treatment zone. Although a longer treatment time is good for microbial inactivation, it also increases the heating impact and may impact other juice's quality characteristics. Therefore, a uniform distribution of the velocity profile implies homogeneous treatment and temperature distribution.

D. TEMPERATURE DISTRIBUTION INSIDE THE TREATMENT ZONE

As time-independent distribution changes from inner-electrode toward outer-electrode, so provides no meaningful information. The insulators placed inside the treatment zone improves the electric field distribution by controlling the laminar flow.

The temperature distribution in the treatment zone depends on the treatment zone's electrical resistance, frequency, pulse width, electrical field distribution, and the treatment area's flow pattern. Therefore, it is not unusual that the insulator's geometry significantly affects the fluid's heating and temperature distribution.

The heat capacity for orange juice was set at 3.73 kJ/ml.°C. Thus, the electrical energy absorbed by juice was ultimately converted to heat. The temperature of the treated juice sample rose by about 7 °C under these circumstances, and a comparable result is shown in Figure 12. It can be seen that the temperature is lowest near the entry point of the tube (r = 0) and increases towards the exit valve. Figure 12 shows a 20 °C temperature at the inlet, and after the treatment, the temperature increased to 27 °C at the outlet point.

IV. SYSTEM DEVELOPMENT

The conductivity of orange juice (0.343 S/m) in the proposed chamber provides a total resistance of 5 Ω. For this purpose, a pulsed power generator of 5 kV, 1.0 kA may produce the necessary electrical field of 10 kV/cm. Figure 13 displays the

FIGURE 12. Simulated result showing temperature (°C) distribution in the treatment zone.

Marx bank generator's single-stage design. When the IGBT gate signals are ready, a pulsed power generator with 5 kV and 1.0 kA output power may be used to upload the DC link voltage to the treatment chamber contained orange juice.

Energy per pulse $= V^*_{out} I^*_{out} PW = 5$ kV$*1$ kA$*3 \mu$ sec $= 15$ J/pulse

The system's total energy (J/sec) can be determined using the energy applied per unit of volume and the liquid's flow rate.

Total energy per second = Energy per volume * Max. flow rate

J. sec $^{-1} = 200$ J.mL^{-1} * 100 mL. sec$^{-1} = 20$ kJ. sec^{-1}

Frequency $= 20$ kJ. sec$^{-1} \times 15$ J. pulse$^{-1} = 1.3$ kHz

Thus, residence time of the liquid inside the treatment zone can be calculated as follows:

Residence time (sec) = Liquid volume in treatment zone/liquid flow rate $= 26$ mL/100 mL.sec$^{-1} = 0.258$ sec

Number of pulses = Residence time (sec) * Pulse frequency (Hz) $= 0.258$ sec * 1.3 kHz $= 335$

Error! Reference Source Not Found: 14 shows the oscilloscope snapshot of the output pulse waveform. As can be observed, the prototype circuit effectively affects parasite inductance and capacitance. Therefore, the output pulse

FIGURE 13. A schematics for a single stage of Marx bank generator.

waveform is not according to the simulation result. It generated a pulse width of 4 μs with a load of 5 Ω. The peak voltage is 4.2 ± 0.2 kV. Figure 15 shows the whole experimental setup of the electroporator with the continuous liquid flow and DE waveform for orange juice treatment. There is a coaxial treatment chamber, a three-stage Marx bank, high voltage DC power supply, a liquid flow controller and a Picoscope oscilloscope.

V. TESTING THE DESIGNED ELECTROPORATOR

Temperature distribution in the treatment chamber is important to achieve better efficiency of a PEF treatment and strike a balance between energy input and high-quality output. Real-time temperature monitoring provides important information regarding the dynamics of chamber temperature rise during the PEF process. However, the relative diameters of the treatment chambers and the temperature measuring apparatus make it challenging to conduct appropriate measurements at different treatment chamber locations without interfering with the flow. In this study, the real-time temperature across the radial axis was monitored using an infrared camera.

FIGURE 14. Output waveform of Marx generator across the treatment chamber filled with orange juice.

A FLIR-SC500 infrared camera with thermal-vision acquisition software (ThermaCAM^{TM} Researcher 2.8 Pro) was used to capture the chamber's temperature distribution. The non-contact type of temperature measurement made it possible to continuously record the temperature changes during the entire treatment. Figure 16 illustrates temperature distribution at various flow rates in the treated orange juice sample. The medium temperature increased over time as more energy was pushed from the inner high-voltage electrode to the outer ground electrode via the radial axis. Thus, it illustrates the temperature distribution at two different flow rates and the temperature drops as the fluid flow rises (figure 16(a).

The medium temperature increased over time as more energy was pushed from the inner high-voltage electrode to the outer ground electrode via the radial axis. Figure 17 illustrates the temperature distribution at two different flow rates and the temperature drops as the fluid flow rise (Figure 16(a). Figure 16 shows the temperature rose over time from the

FIGURE 15. Experimental setup of electroporator with continuous liquid flow and double-exponential waveform for orange juice treatment.

inner high-voltage electrode to the outer ground electrode, increasing the sample juice's temperature by 7 °C above the ambient. The temperature distribution in the treatment region was confirmed by images taken at two different flow speeds, and the temperature falls as the liquid flow increases. Therefore, a high flow rate is suggested since it limits the temperature rise and associated adverse effects to a minimum.

Figure 17 shows a physical appearance of the untreated (S0), thermally treated (S1, 65°C, 30 min), and PEF treated (S2) orange juice samples at different days; (17.a) day 0, (17.b) after storage of 9 days at 4 °C. Over time, the colour change in treated orange juice reduces shelf life quality. This is the first indication that consumers may have a problem. Colour changes may occur in response to the production of brown pigments and the fading of carotenoids, the naturally occurring pigments in orange juice. Table 3 shows the variation in the colour parameters, a*, b* and L*. The overall trend for the colour of orange juices during storage time showed that lightness (L* value) decreased, redness (a* value) increased., and yellowness (b* value) decreased. There are no significant differences in colour parameters between thermally treated and untreated orange juice. In contrast, PEF treated orange juice shows differences for all L*, a* and b* values directly after production. A colour shift toward positive b* and negative a*. The majority of samples show a more decrease in CIE L* value after, indicating a darkling

of juice surface colour. A slight increase in CIE L* value from 40.1 ± 0.37 to 39.4 ± 0.43 for pasteurised juices can probably be attributed to partial precipitation of unstable, suspended particles in juice.
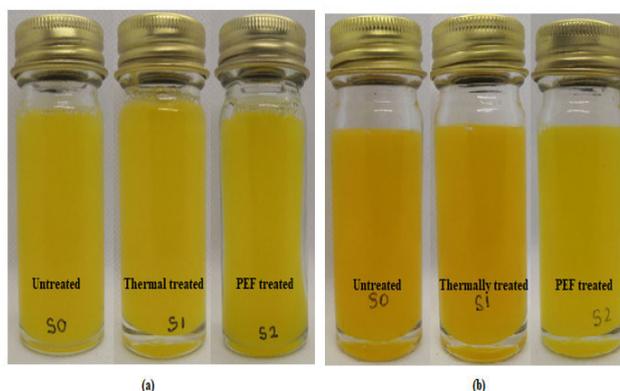
FIGURE 17. Physical appearance of the untreated, thermally treated, and PEF treated orange juice samples at different days; (a) day-0, (b) after storage of 9 days at 4 °C.

The total colour differences ($\Delta E^* = [(\Delta L^*)^2 + (\Delta a^*)^2 + (\Delta b^*)^2]^{1/2}$) of untreated samples (S0), thermally treated (S1) and PEF treated(S2), were calculated as 3.98, 3.59 and 0.75. Based on the measured ΔE values, it was discovered that untreated and thermally treated juice samples exhibited a colour change compared to PEF treatment samples, which showed minor colour changes.

Total Viable Counts (TVCs) is a general bacteria test to measure the total amount of food-containing microorganisms. Untreated, thermal, and PEF treated juice samples in triplicate were subjected to a microbial test (Total Viable Count, TVC) at the Institute of Bioproduct Development, UTM. A standard technique, Microbial Contamination BP 2008, Volume IV, Appendix XVI B, was used to analyse the total plate count in triplicate. The total number of colonies to determine Total Plate Count was counted as follows: (a) Following incubation, exam the plates for growth, count those plates on which less than 300 cfu, and express the average for
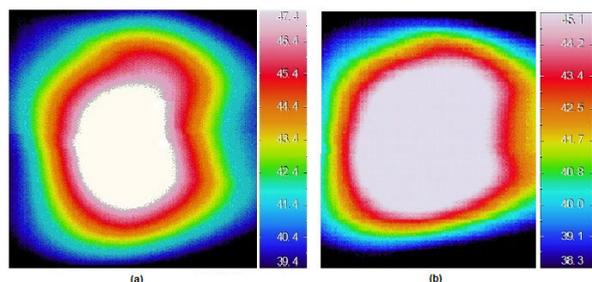
FIGURE 16. Real-time temperature distribution in the treated orange juice under different flow rates; (a) 50 ml/sec (b) 10 ml/sec.

TABLE 3. Colour L*, a* and b* of samples at day 0 and 9.

Parameter	Sample	0 Day	9th Days
L*	Untreated	40.31±0.08	36.41±0.06
	Thermally treated	41.46±0.04	37.94±0.03
	PEF treated	40.12±0.05	39.4±0.05
a*	Untreated	2.04±0.04	2.63±0.26
	Thermally treated	2.13±0.09	2.54±0.03
	PEF treated	2.18±0.03	2.36±0.12
b*	Untreated	27.04±0.07	26.48±0.41
	Thermally treated	27.17±0.05	26.61±0.85
	PEF treated	27.07±0.06	26.95±0.09

TABLE 4. Total viable count in untreated, thermal and PEF treated samples with and without sieves at different times.

Sample	0 Day	9th Days
Untreated		230±28
Thermally treated		16±5
PEF treated without sieves	<10	17±2
PEF treated with sieves		16±3

the two plates in terms of the number of cfu/gm or cfu/ml of sample. (b) Use a colony counter to register the count and mark the counted colonies to avoid recounting. (c) If no microbial colonies are recovered from dishes representing the initial 1:10 dilution of the sample, express the result as "less than 10 cfu/gm or 10 cfu/ml" of the sample.

The TVC was performed on all four samples after 9 days of storage. Although the sample was kept at 4°C, the colony's vitality was enhanced to 230 ± 28 cfu/ml in an untreated sample. After 9 days of storage, the TVC in the PEF treated sample was similar to that of thermally treated samples, with 16 ± 5 cfu/ml. As expected, a PEF treated sample with sieves shows a slightly better result (16 ± 3 cfu/ml) than another PEF treated sample without sieves (17 ± 2 cfu/ml). As a result, the electroporator was found to be suitable for microbial inactivation.

VI. CONCLUSION

This research aims to describe the process of creating the specialised equipment required for liquid food pasteurisation. The electrical system's complexity impedes the development of this innovation for continuous processing in an industrial environment. A pulsed-power generator and a treatment chamber are critical PEF pasteurisation equipment. The procedure parameters are based on the pulsed power generator and the treatment chamber characteristics. A new coaxial treatment chamber was proposed to avoid the flashover and provide a more uniform field distribution via turbulence flow. In the simulation research, COMSOL Multiphysics monitored a uniform velocity profile in the treatment zone. The proposed treatment chamber was fabricated, and initial calculations for the pulsed power supply's design was done. The double-exponential waveform was found to be more effective than the ED waveform in liquid food pasteurisation.

It lowers system power losses as more power is required in case of ED. A Marx generator based on the IGBT was built to produce a DE waveform for the proposed treatment chamber. The whole design system was put through a trial set to verify its effectiveness in pasteurising orange pasteurisation. The treated samples demonstrated that the designed electroporator successfully preserved the treated food samples' microbiologic stability and colour. Its performance was better than that using the thermal procedure. This research offers important results in developing and using PEF-based food treatment to inactivate microorganisms, especially at low liquid flow speed.

REFERENCES

[1] R. N. Arshad, Z. Abdul-Malek, U. Roobab, M. I. Qureshi, N. Khan, M. H. Ahmad, Z. Liu, and R. M. Aadil, "Effective valorization of food wastes and by-products through pulsed electric field: A systematic review," *J. Food Process Eng.*, vol. 44, no. 3, Mar. 2021, Art. no. e13629.

[2] A. Režek Jambrak, M. Nutrizio, I. Djekiá, S. Pleslić, and F. Chemat, "Internet of nonthermal food processing technologies (IoNTP): Food industry 4.0 and sustainability," *Appl. Sci.*, vol. 11, no. 2, p. 686, Jan. 2021.

[3] M. Gavahian, N. Pallares, F. Al Khawli, E. Ferrer, and F. J. Barba, "Recent advances in the application of innovative food processing technologies for mycotoxins and pesticide reduction in foods," *Trends Food Sci. Technol.*, vol. 106, pp. 209–218, Dec. 2020.

[4] R. N. Arshad, Z. Abdul-Malek, U. Roobab, M. A. Munir, A. Naderipour, M. I. Qureshi, Z.-W. Liu, and R. M. Aadil, "Pulsed electric field: A potential alternative towards a sustainable food processing," *Trends Food Sci. Technol.*, vol. 111, pp. 43–54, May 2021.

[5] R. N. Arshad, Z. Abdul-Malek, A. Munir, Z. Buntat, M. H. Ahmad, Y. M. M. Jusoh, A. E.-D. Bekhit, U. Roobab, M. F. Manzoor, and R. M. Aadil, "Electrical systems for pulsed electric field applications in the food industry: An engineering perspective," *Trends Food Sci. Technol.*, vol. 104, pp. 1–13, Oct. 2020.

[6] N. F. Kasri, M. A. M. Piah, and Z. Adzis, "Compact high-voltage pulse generator for pulsed electric field applications: Lab-scale development," *J. Electr. Comput. Eng.*, vol. 2020, Sep. 2020, Art. no. 6525483.

[7] M. A. Elgenedy, A. Darwish, S. Ahmed, and B. W. Williams, "A modular multilevel generic pulse-waveform generator for pulsed electric field applications," *IEEE Trans. Plasma Sci.*, vol. 45, no. 9, pp. 2527–2535, Sep. 2017.

[8] S. El Kantar, N. Boussetta, N. Lebovka, F. Foucart, H. N. Rajha, R. G. Maroun, N. Louka, and E. Vorobiev, "Pulsed electric field treatment of citrus fruits: Improvement of juice and polyphenols extraction," *Innov. Food Sci. Emerg. Technol.*, vol. 46, pp. 153–161, Apr. 2018.

[9] K. Knoerzer, P. Baumann, and R. Buckow, "An iterative modelling approach for improving the performance of a pulsed electric field (PEF) treatment chamber," *Comput. Chem. Eng.*, vol. 37, pp. 48–63, Feb. 2012.

[10] F. Schottroff, J. Knappert, P. Eppmann, A. Krottenthaler, T. Horneber, C. McHardy, C. Rauh, and H. Jaeger, "Development of a continuous pulsed electric field (PEF) vortex-flow chamber for improved treatment homogeneity based on hydrodynamic optimization," *Frontiers Bioeng. Biotechnol.*, vol. 8, p. 340, Apr. 2020.

[11] H. Masood, Y. Diao, P. J. Cullen, N. A. Lee, and F. J. Trujillo, "A comparative study on the performance of three treatment chamber designs for radio frequency electric field processing," *Comput. Chem. Eng.*, vol. 108, pp. 206–216, Jan. 2018.

[12] H. Jaeger, N. Meneses, and D. Knorr, "Impact of PEF treatment inhomogeneity such as electric field distribution, flow characteristics and temperature effects on the inactivation of E. coli and milk alkaline phosphatase," *Innov. Food Sci. Emerg. Technol.*, vol. 10, no. 4, pp. 470–480, 2009.

[13] L. Buchmann, R. Bloch, and A. Mathys, "Comprehensive pulsed electric field (PEF) system analysis for microalgae processing," *Bioresource Technol.*, vol. 265, pp. 268–274, Oct. 2018.

[14] J. Raso, W. Frey, G. Ferrari, G. Pataro, D. Knorr, J. Teissie, and D. Miklavä, "Recommendations guidelines on the key information to be reported in studies of application of PEF technology in food and biotechnological processes," *Innov. Food Sci. Emerg. Technol.*, vol. 37, pp. 312–321, Oct. 2016.

[15] S. Jegatheeswaran, F. Ein-Mozaffari, and J. Wu, "Process intensification in a chaotic SMX static mixer to achieve an energy-efficient mixing operation of non-newtonian fluids," *Chem. Eng. Process. Intensification*, vol. 124, pp. 1–10, Feb. 2018.

[16] R. N. Arshad, Z. B. Buntat, A. M. Dastgheib, Y. M. M. Jusoh, A. Munir, R. M. Aadil, and M. H. Ahmad, "Continuous flow treatment chamber for liquid food processing through pulsed electric field," *J. Comput. Theor. Nanoscience*, vol. 17, no. 2, pp. 1492–1498, Feb. 2020.

[17] M. Kandušer, A. Belicč, S. čorovič, and I. Škrjanc, "Modular serial flow through device for pulsed electric field treatment of the liquid samples," *Sci. Rep.*, vol. 7, no. 1, Dec. 2017, Art. no. 8115.

[18] S. H. Jayaram, "Sterilisation of liquid foods by pulsed electric fields," *IEEE Electr. Insul. Mag.*, vol. 16, no. 6, pp. 17–25, Nov. 2000.

[19] A. M. Hodgins, G. S. Mittal, and M. W. Griffiths, "Pasteurization of fresh orange juice using low-energy pulsed electrical field," *J. Food Sci.*, vol. 67, no. 6, pp. 2294–2299, Aug. 2002.

[20] R. Buckow, S. Schroeder, P. Berres, P. Baumann, and K. Knoerzer, "Simulation and evaluation of pilot-scale pulsed electric field (PEF) processing," *J. Food Eng.*, vol. 101, no. 1, pp. 67–77, Nov. 2010.

[21] R. N. Arshad, Z. Abdul-Malek, and M. H. Ahmad, "Coaxial treatment chamber for liquid food treatment through pulsed electric field," *Indonesian J. Electr. Eng. Comput. Sci.*, vol. 19, no. 3, pp. 1169–1176, 2020.

[22] O. Parniakov, F. J. Barba, N. Grimi, N. Lebovka, and E. Vorobiev, "Impact of pulsed electric fields and high voltage electrical discharges on extraction of high-added value compounds from papaya peels," *Food Res. Int.*, vol. 65, pp. 337–343, Nov. 2014.

[23] H. Meng, M. Song, Y. Yu, F. Wang, and J. Wu, "Chaotic mixing characteristics in static mixers with different axial twisted-tape inserts," *Can. J. Chem. Eng.*, vol. 93, no. 10, pp. 1849–1859, Oct. 2015.

[24] H. Meng, M. Han, Y. Yu, Z. Wang, and J. Wu, "Numerical evaluations on the characteristics of turbulent flow and heat transfer in the lightnin static mixer," *Int. J. Heat Mass Transf.*, vol. 156, Aug. 2020, Art. no. 119788.

[25] A. Ghanem, T. Lemenand, D. Della Valle, and H. Peerhossaini, "Static mixers: Mechanisms, applications, and characterisation methods-A review," *Chem. Eng. Res. Design*, vol. 92, no. 2, pp. 205–228, 2014.

[26] M. S. Moonesan and S. H. Jayaram, "Effect of pulsewidth on medium temperature rise and microbial inactivation under pulsed electric field food treatment," *IEEE Trans. Ind. Appl.*, vol. 49, no. 4, pp. 1767–1772, Jul. 2013.

[27] H. Masood, A. Razaeimotlagh, P. J. Cullen, and F. J. Trujillo, "Numerical and experimental studies on a novel steinmetz treatment chamber for inactivation of Escherichia coli by radio frequency electric fields," *Innov. Food Sci. Emerg. Technol.*, vol. 41, pp. 337–347, Jun. 2017.

[28] J. M. Martínez, E. Luengo, G. Saldaña, I. Álvarez, and J. Raso, "C-phycocyanin extraction assisted by pulsed electric field from artrosphira platensis," *Food Res. Int.*, vol. 99, pp. 1042–1047, Sep. 2017.

[29] R. N. Arshad, Z. Buntat, M. A. B. Sidik, A. Alamgir, Z. Nawawi, and M. Hafizi, "Proficiency of double-exponential pulse waveform in food treatment through pulsed electric field," in *Proc. 2nd Int. Conf. High Voltage Eng. Power Syst. (ICHVEPS)*, Oct. 2019, pp. 218–222.

ZULKURNAIN ABDUL-MALEK (Senior Member, IEEE) received the B.E. degree in electrical and computer systems from Monash University, Melbourne, VIC, Australia, in 1989, the M.Sc. degree in electrical and electromagnetic engineering from the University of Wales Cardiff, Cardiff, U.K., in 1995, and the Ph.D. degree in high voltage engineering from Cardiff University, U.K., in 1999. He is currently a Professor with the Faculty of Engineering, School of Electrical, Universiti Teknologi Malaysia. He is also working as a Professor and the Director of the Institute of High Voltage and High Current (IVAT), University of Technology Malaysia (UTM), Johor Bahru, Malaysia. He has more than 150 international conference and journal publications along with 40 copyrights and patents. His research interests include ageing and condition monitoring of surge arresters and power transformers, partial discharge measurement, high voltage and high current transducers, and insulating material testing and coordination.

ABDULLAH MUNIR received the bachelor's and master's degree in electrical engineering from the NED University of Engineering and Technology, Karachi, Pakistan, in 2011 and 2014, respectively. He is currently pursuing the Ph.D. degree with the Institute of High Voltage and High Current (IVAT), Universiti Teknologi Malaysia (UTM), Johor Bahru, Malaysia, working on the condition monitoring of gapless metal oxide surge arresters. Since 2013, he has been working as a Lecturer with NED University. His research interests include high voltage engineering, condition monitoring and diagnostics of high voltage devices and instruments, energy conservation, and power quality.

MOHD HAFIZI AHMAD (Member, IEEE) received the Ph.D. degree in high voltage engineering from the Institute of High Voltage and High Current (IVAT), University Technology of Malaysia (UTM). He is currently working as a Senior Lecturer and a Researcher with the IVAT, UTM. His Ph.D. works are related to partial discharge measurement on insulation. He has conducted several pieces of training and talks on partial discharge fundamentals and measurement on primary electrical equipment for industries and universities. He is a member of IET UK.

RAI NAVEED ARSHAD received the M.Sc. degree in electronics from Quaid-I-Azam University, Islamabad, and the M.S. degree in systems engineering from Pakistan Institute of Engineering and Applied Sciences (PIEAS), Islamabad. He is currently pursuing the Ph.D. degree in electrical engineering with the Institute of High Voltage and High Current, Universiti Teknologi Malaysia (UTM), Johor, Malaysia. His research interests include power electronics, high-voltage engineering, pulsed power technology, food technologies, and non-thermal processing. He is also developing an electroporator for liquid food treatment.

ZAINUDDIN NAWAWI currently works with the Electrical Department, Universitas Sriwijaya. His current project is lightning detection system and application plasma technology for sterilisation of surgery equipment. His research interests include electrical engineering, materials science, and materials physics.

MUHAMMAD ABU BAKAR SIDIK (Member, IEEE) is currently an Associate Professor and the Head of the Department of Electrical Engineering, Faculty of Engineering, Universitas Sriwijaya.

HAMMAD ALOTAIBI received the Ph.D. degree in mathematics from Adelaide University, Australia, in 2017. He has published several research articles in different well-reputed international journals. His research interests include modeling complex multi-scale dynamical systems, atomic simulation, and numerical and analytical computational methods for solving differential equations.

TOUQEER A. JUMANI received the Ph.D. degree from Universiti Teknologi Malaysia, in October 2020. He is currently working as an Assistant Professor with the Department of Electrical Engineering, Mehran UET, SZAB Campus, Khairpur Mir, Pakistan. His research interests include power quality, grid integration of renewable sources, dynamic response enhancement, and swarm intelligence-based optimization.

ILYAS KHAN received the Ph.D. degree in applied mathematics from the Universiti Teknologi Malaysia (UTM), Malaysia. He has around 15 years of academic experience in different reputed institutions of the world. He is currently an Associate Professor with the Department of Mathematics, College of Science, Majmaah University, Saudi Arabia. He has published more than 700 research articles in different well-reputed international journals. His research interests include mathematical modeling, analytical and computational fluid dynamics, bio-mathematics, and numerical computing.

AFRASYAB KHAN received the master's degree in physics, the master's degree in materials science in power engineering, and the Ph.D. degree in chemical engineering from the Universiti Malaysia Sarawak (UNIMAS). He is currently working with the Department of Hydraulics and Hydraulic and Pneumatic Systems, Faculty of Mechanical Engineering, South Ural State University, Chelyabinsk, Russian. He is an Active Member of the Institution of Mechanical Engineers (MIMechE).

. . .